



Optimization of High-Sensitivity SQUID Gradiometer for ARIADNE at CAPP

Violeta Gkika¹ · Younggeun Kim¹ · Andrei Matlashov¹ · Yun Chang Shin¹ ·
Yannis Semertzidis¹ · Robin Cantor² · Chloe Lohmeyer³ · Nancy Aggarwal³ ·
Andrew Geraci³

Received: 1 November 2023 / Accepted: 30 April 2024 / Published online: 22 May 2024
© The Author(s), under exclusive licence to Springer Science+Business Media, LLC, part of Springer Nature
2024

Abstract

ARIADNE (Axion Resonant InterAction Detection Experiment) is a table-top experiment that intends to search for QCD axions from exotic spin-dependent interactions mediated by axion between nuclei at sub-mm range. This experiment includes a non-magnetic mass to source the axion field, and a dense ensemble of hyper-polarized ${}^3\text{He}$ nuclei to detect the axion field with nuclear-magnetic-resonance (NMR)-based method. The expected NMR signal from the interaction could be easily buried in the noise spectrum of the magnetometer, especially in a frequency range (~ 100 Hz) where the interaction signal is supposed to exist. In this work, we report optimization of SQUID gradiometer for ARIADNE including noise spectrum measurement.

Keywords Axions · ARIADNE · NMR · ${}^3\text{He}$ · SQUID

1 Introduction

The axion is a hypothetical pseudo-scalar boson postulated in the 1970s by Peccei and Quinn (PQ) to solve the strong-CP problem in quantum chromodynamics (QCD) [1–3]. It provides a dynamical mechanism to explain the smallness of the neutron's electric dipole moment [2]. Axion can also be a leading candidate to explain the dark matter in our universe due to their invisible nature [4]. Direct search for axions from axion to photon conversion in a resonant cavity is the intent of many

✉ Violeta Gkika
violeta@ibs.re.kr

¹ Center for Axion and Precision Physics Research, Institute for Basic Science, Daejeon, Republic of Korea

² Star Cryoelectronics, Santa Fe, NM, USA

³ Department of Physics, Northwestern University, Evanston, IL, USA

of those axion experiments such as CAPP-MAX or ADMX [5, 6]. In addition to the interaction with photons, axions can couple to fundamental fermions through scalar and pseudo-scalar vertices which violates P and T symmetry [3, 7]. This interaction can be tested in laboratory experiments when detecting coherent field from many particles simultaneously.

ARIADNE (Axion Resonant InterAction Detection Experiment) is a table-top experiment that intends to search for QCD axions from exotic spin-dependent interactions between an unpolarized source mass and a spin-polarized ^3He . This interaction between nuclei is supposed to be mediated by axion at sub-mm range with a potential energy given by

$$U_{\text{sp}}(r) = \frac{\hbar^2 g_s^N g_p^N}{8\pi m_f} \left(\frac{1}{r\lambda_a} + \frac{1}{r^2} \right) e^{-\frac{r}{\lambda_a}} (\hat{\sigma}, \hat{r}) \quad (1)$$

where g_s and g_p are the monopole and dipole coupling constants, respectively, m_f is the fermion mass, $\hat{\sigma}$ is the Pauli spin matrix, \hat{r} is the vector between them, and λ_a is the Compton wavelength of axion which determines the range over which the interaction extends [7, 8]. For the QCD axion, the scalar and pseudo-scalar coupling constants g_s^N and g_p^N are directly correlated to the axion mass. Since the axion couples to $\hat{\sigma}$, which is proportional to the magnetic moment $\vec{\mu}_N$ of the nucleus, the axion coupling in this interaction can be expressed as a fictitious magnetic field B_{eff} as one can treat Eq. 1 as $U_{\text{sp}}(r) = -\vec{\mu}_N \cdot \vec{B}_{\text{eff}}$ [9].

As the polarized ^3He NMR sample resides in an external magnetic field of $B_{\text{ext}} \sim 30\text{mG}$, the transverse magnetic field B_{eff} drives spin precession in the polarized ^3He which is accumulated over the T_2 time of ^3He and eventually cause a shift of Larmor precession frequency. This could be detected by placing a high-sensitive magnetometer such as SQUID behind the ^3He sample. In this case, the ^3He sample acts as an amplifier to transduce the small effective magnetic field into a larger real magnetic field detectable by the SQUID. The experiment uses a resonant enhancement technique and, in principle, allows several orders of magnitude improvement, yielding sufficient sensitivity to detect the QCD axion as shown in Fig. 1 [10].

However, in the real case, the total noise spectrum of SQUID magnetometer could be easily affected from (filled up with) the environmental background noise, such as acoustic and vibration noises, especially in a frequency range below 100 Hz. In this paper, a SQUID-based co-centric planar gradiometer was tested in an attempt to resolve this problem which eventually leads to improve the SQUID sensitivity.

2 Comparison of SQUID Magnetometer and Gradiometer

The fundamental noise source which will limit ARIADNE's sensitivity is the quantum noise caused by the transverse spin projection in the ^3He . The minimum magnetic field due to the magnetization from quantum fluctuation of the spin system is estimated as $3 \times 10^{-19}\text{T}/\sqrt{\text{Hz}}$ for $T_2 = 1000\text{sec}$. In order to sense the axion

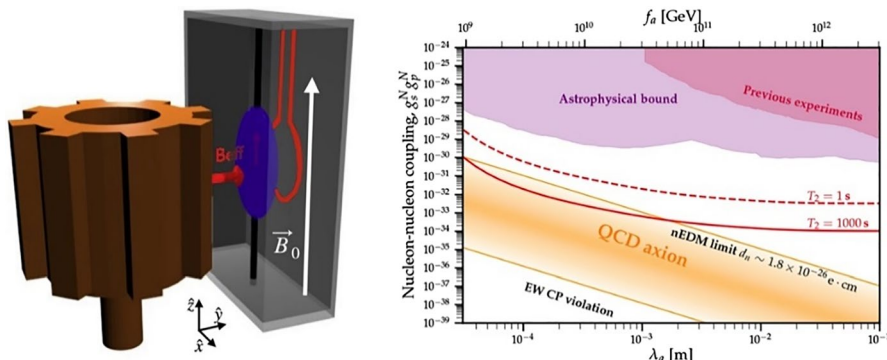


Fig. 1 Left: Setup: A sprocket-shaped source mass is rotated so its “teeth” pass near an NMR sample at its resonant frequency. Right: Projected reach for monopole–dipole axion-mediated interactions. The band bounded by the red (dark) solid line and dashed line denotes the limit set by transverse magnetization noise, depending on achieved T_2 . Constraints and expectations for the QCD axion are also shown

induced magnetic field, therefore, the SQUID noise level should be close to the level of $2fT/\sqrt{\text{Hz}}$ at 100 Hz. However, it is a laborious task to maintain this level of sensitivity with SQUID magnetometer in the real setup of ARIADNE for the following reasons. First of all, the SQUID magnetometer must be located in close proximity to the polarized ^3He ensemble. But, at the same time, the pickup loop has high influence from the external magnetic holding field B_{ext} even with a small misalignment with an arbitrary angle. Second, the magnetometer itself is very sensitive even to acoustic noise from the environment. For example, with a $1\text{nm}/\sqrt{\text{Hz}}$ vibration, about $3\text{pT}/\sqrt{\text{Hz}}$ of noise could be induced at the pickup coil with 3-mm diameter. Those will eventually become dominant noise source in ARIANDE experiment regardless of the low intrinsic noise of magnetometer. For this reason, a configuration of SQUID gradiometer is considered to be more effective for the effective suppression of background fields even from distant sources while retaining substantially high sensitivity to the nearby magnetic field sources [11].

A setup of the gradiometer configuration has been tested and compared with the magnetometer in terms of noise reduction. The gradiometer setup has been emulated with two SQUID magnetometers and an electric compensation circuit. Between two SQUIDs, one is connected to the inner double-turn pickup loop with radius $R_{in} = 7\text{mm}$ (inner pickup coil) and the other is connected to the outer single-turn pickup loop with radius $R_{out} = 7\sqrt{2}\text{mm}$ (compensation coil) wound with opposite helicity. An additional coil is attached 2 mm below the inner pickup loop to generate a dipole field near the gradiometer system. Each coil is connected to the separate SQUID magnetometer, and the compensation of signal from each SQUID is processed with an electric compensation circuit which mimics the function of SQUID gradiometer as shown in Fig. 2 (Left) [12]. The noise spectral densities from each magnetometer and gradiometer circuit were measured by using a spectrum analyzer up to 200 Hz frequency range over 10^4 averaging cycles as shown in Fig. 2 (Right). Noise levels from inner and outer coils show almost identical behavior over

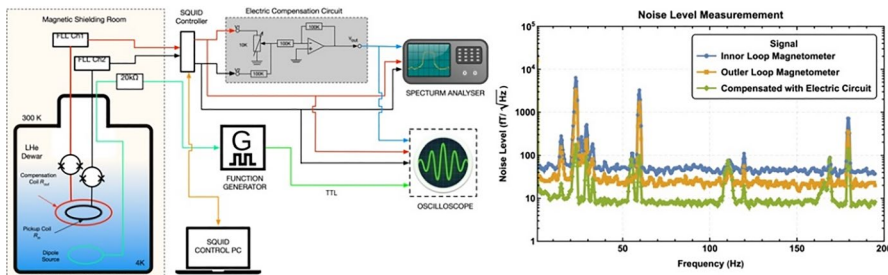


Fig. 2 Left: A schematic for testing the noise compensation performance of SQUID gradiometer with magnetometer. Inner and outer compensation pickup loops are wound with opposite helicity. Right: The noise power spectral density measured from each magnetometer as well as the electric compensation circuit

the frequency range while the noise density from the gradiometer setup is much lower than those levels. It indicates that gradiometer effectively compensates background noise field applied to both magnetometers.

3 Optimization of SQUID Gradiometer

The FEM (Finite Element Method) study of SQUID gradiometer was done with COMSOL to identify the optimal gradiometer configuration. In this study, the flux generated from the polarized ^3He and the intrinsic noise are estimated as a function of the pickup loop radius of the gradiometer as well as the distance between the coil and the superconducting wall z_0 as shown in Fig. 3. The pickup loop radius was identified with a way to maximize the signal-to-noise ratio $\text{SNR} = \phi_g / \sqrt{\delta\phi_g}$ where $\delta\phi_g$ is the intrinsic noise of the gradiometer and ϕ_g is flux induced by local dipole source. For the gradiometer, the possible noise sources may come from intrinsic noise, vibrational-induced noise, and NMR spin quantum fluctuation-induced noise.

Through the optimization process with FEM, the size of the gradiometer pickup coils has been chosen as $R_{\text{in}} = 1.725\text{mm}$, 1.785 mm and $R_{\text{out}} = 2.5\text{mm}$ for the first inner, second inner and outer (compensate) radius, respectively, with considering its reduced noise and the sensitivity of the experiment. The design and fabrication of

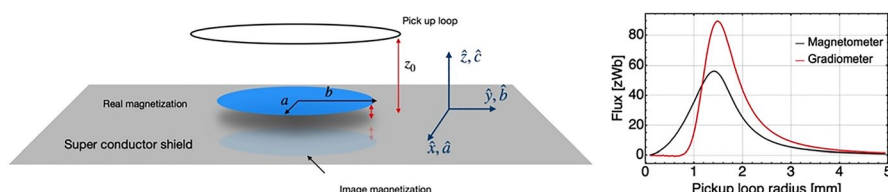


Fig. 3 Left: The transverse magnetization is estimated by means of FEM method from the fictitious magnetic field generated by the spin-dependent interaction between the polarized ^3He and rotating mass. Right: Estimated magnetic flux depending on the pickup loop radius for magnetometer and gradiometer design with pickup loop at $z_0 = 0.5\text{ mm}$

gradiometer have been outsourced to STAR Cryoelectronics with utilization of the thin-film technology based on the optimized dimensions from the FEM study. Figure 4 (Right) shows the SQUID gradiometer fabricated from the manufacturer. The characterization of the SQUID gradiometer has been made at CAPP after receiving them, and a schematic of the test setup for the SQUID test is shown in Fig. 4 (Left). A set of measurements have been done using an external (dipole) coil placed at a distance 4mm from the gradiometer pickup coil (Middle). With the function generator connected to the ring dipole, the measurements of the voltage to magnetic field ratio calibration have been done.

A measurement of the SQUID response was done as a function of input voltages.

Sinusoidal voltage signal was driven to the dipole coil from a function generator of 2 V, 4 V, 6 V, 8 V, and 10 V, respectively, to drive the flux to the SQUID. The dipole coil was located behind of the pickup loop with a distance of 4 mm.

The ratio of the magnetic flux density through the pickup coil to the output response voltage of SQUID can be evaluated as $B_V = B_{in}/V_{out}$ (Table 1), where B_{in} is the magnetic flux density estimated from COMSOL simulations of dipole field at the level of pickup coil, and V_{out} the response output voltage displayed in the oscilloscope. The spectral voltage noise power density at the output of the FLL, S_V , was measured in order to determine the intrinsic noise of the SQUID as well as electronic associated with it. A spectral-power density of the flux noise, S_ϕ , was estimated as $S_\phi^{1/2} = S_V^{1/2} / V_\phi (\phi_0 / \sqrt{\text{Hz}})$ where $V_\phi = \partial V_{out} / \partial \phi_0$ is the transfer function which is defined as the ratio of the signal output to the flux applied to the SQUID. This can be achieved by displaying the SQUID voltage against applied flux by measuring the peak-to-peak voltage on an oscilloscope. The transfer function for this measurement was set by $V_\phi = 2.8V/\phi_0$.

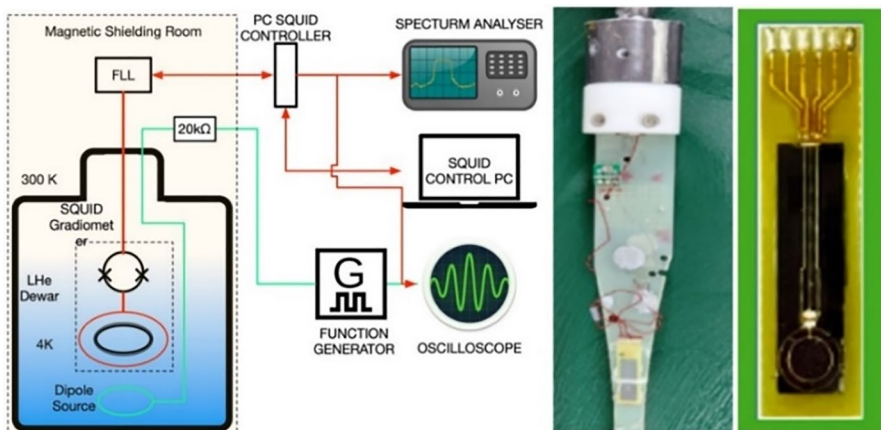


Fig. 4 Left: Schematic view of the experimental setup for the SQUID gradiometer test measurements. The gradiometer surrounded by the lead shield is inserted directly into the helium Dewar. A dipole coil (green) is connected to the function generator. Middle: Image of the probe where the sensor is located. Right: Close view of the sensor from probe installed in the PCB

Table 1 A set of measurements and simulations for the system calibration

$V_{\text{in}}[\text{V}]$	$V_{\text{out}}[\text{V}]$	$R[\text{k}\Omega]$	$B_{\text{in}}[\text{T}]$	$B_V[\text{TV}^{-1}]$
2	0.38	20	4.14×10^{-9}	1.0799×10^{-8}
4	0.72	20	9.03×10^{-9}	1.2542×10^{-8}
6	1.11	20	1.35×10^{-8}	1.2162×10^{-8}
8	1.45	20	1.81×10^{-8}	1.2480×10^{-8}
10	1.84	20	2.26×10^{-8}	1.2282×10^{-8}

V_{in} is the input voltage from a function generator, V_{out} the response output voltage displayed in the oscilloscope, R the resistor through with the dipole source is connected to a function generator, and B_{in} the magnetic flux density through the pickup coil from COMSOL simulations

The spectral voltage noise power density at 100 Hz was measured as $S_V = 15\mu\text{V}_{\text{rms}}/\sqrt{\text{Hz}}$. From above, the measured noise of the thin-film SQUID gradiometer is $S_V \sim 5.4\mu\phi_0/\sqrt{\text{Hz}}$.

4 Conclusions

We studied the SQUID gradiometers in terms of noise reduction for ARIADNE compared with magnetometer. Based on the reduced noise level and sensitivity of signal, a design parameter for a SQUID gradiometer has been chosen. A prototype SQUID gradiometer has been fabricated and tested in terms of sensitivity by measuring the signal from a dipole source. The rms spectral density of field noise was measured at the level of $5.4\mu\phi_0/\sqrt{\text{Hz}}$.

Author contributions V.G. and Y.C.S. wrote the main manuscript. V.G., Y.K., A.M., and Y.C.S. performed the measurements and analyzed the data. R.C. fabricated the SQUID gradiometer. All authors reviewed the manuscript.

Declarations

Conflict of interest The authors declare no competing interests.

References

1. R.D. Peccei, H.R. Quinn, Phys. Rev. Lett. **38**, 1440 (1977)
2. S. Weinberg, Phys. Rev. Lett. **40**, 223 (1978)
3. F. Wilczek, Phys. Rev. Lett. **40**, 279 (1978)
4. P. Gondolo, L. Visinelli, Phys. Rev. Lett. **113**, 011802 (2014)
5. A.K. Yi et al., Phys. Rev. Lett. **130**, 071002 (2023)
6. R. Khatiwada et al., Rev. Sci. Instrum. **92**, 124502 (2021)
7. J.E. Moody, F. Wilczek, Phys. Rev. D **30**, 130 (1984)
8. A. Arvanitaki, A.A. Geraci, Phys. Rev. Lett. **113**, 161801 (2014)

9. H. Fosbinder-Elkins et al., *Quantum. Sci. Technol.* **7**, 014002 (2022)
10. H. Fosbinder-Elkins et al., (2018) Progress on the ARIADNE axion experiment, in *Microwave Cavities and Detectors for Axion Research*. In: *Proceedings of the 2nd International Workshop*, pp. 151–161
11. S. Kuriki et al., *J. Appl. Phys.* **61**, 781 (1987)
12. Y. Kim, PhD thesis, KAIST, Daejeon, Korea, (2021)

Publisher's Note Springer Nature remains neutral with regard to jurisdictional claims in published maps and institutional affiliations.

Springer Nature or its licensor (e.g. a society or other partner) holds exclusive rights to this article under a publishing agreement with the author(s) or other rightsholder(s); author self-archiving of the accepted manuscript version of this article is solely governed by the terms of such publishing agreement and applicable law.